



Localized modes revealed in random lasers

BHUPESH KUMAR,¹ RAN HOMRI,¹ PRIYANKA,¹ SANTOSH K. MAURYA,¹ MELANIE LEBENTAL,² AND PATRICK SEBBAH^{1,3,*}

¹Department of Physics, The Jack and Pearl Resnick Institute for Advanced Technology, Bar-Ilan University, Ramat-Gan, 5290002, Israel

²Laboratoire Lumière, matière et interfaces (LuMin) ENS Paris-Saclay, CNRS, Université Paris-Saclay, CentraleSupélec, 91190, Gif-sur-Yvette, France

³Institut Langevin, ESPCI ParisTech CNRS UMR7587, 1 rue Jussieu, 75238 Paris Cedex 05, France

*Corresponding author: patrick.sebbah@biu.ac.il

Received 19 April 2021; revised 17 June 2021; accepted 19 June 2021 (Doc. ID 428217); published 26 July 2021

In sufficiently strong scattering media, light transport is suppressed and modes are exponentially localized. Anderson-like localized states have long been recognized as potential candidates for high- Q optical modes for low-threshold, cost-effective random lasers. Operating in this regime remains, however, a challenge since Anderson localization is difficult to achieve in optics, and nonlinear mode interaction compromises its observation. Here, we exhibit individually each lasing mode of a low-dimension solid-state random laser by applying a non-uniform optical gain. By undoing gain competition and cross-saturation, we demonstrate that all lasing modes are spatially localized. We find that selective excitation significantly reduces the lasing threshold, while lasing efficiency is greatly improved. We show further how their spatial locations are critical to boost laser power efficiency. By efficiently suppressing the spatial hole burning effect, we can turn on the optimally outcoupled random lasing modes. Our demonstration opens the road to the exploration of linear and nonlinear mode interactions in the presence of gain, as well as disorder-engineering for laser applications. © 2021 Optical Society of America under the terms of the [OSA Open Access Publishing Agreement](#)

<https://doi.org/10.1364/OPTICA.428217>

1. INTRODUCTION

Light transport in strongly scattering disordered systems is governed by the nature of the underlying eigenmodes, more specifically, their spatial extension within the scattering medium. For sufficiently strong disorder, the modes of vibration become spatially confined and transport is impeded. Disorder-induced localization is one of the most striking and puzzling manifestations of wave interference, predicted by P.W. Anderson for electrons [1] and later generalized to classical waves [2,3]. If Anderson localization in three-dimensional photonics has never been demonstrated and its very existence is today in question [4], optical localization in lower dimensions is possible for sufficiently large disordered systems. A major challenge, however, in the study of Anderson-like localized states in low-dimensional optical systems resides in the difficulty to excite them independently and observe them individually. Only in the particular situation of extremely strong scattering where modes are well separated and long-lived have localized modes been observed individually in optics [5].

A possible route suggested theoretically to overcome this difficulty is to introduce gain and investigate rather random lasing modes [6,7]. The observation of sharp lasing peaks in semiconductor powders [8] has triggered interest in random lasers, raising the question of the origin of laser oscillations and the nature of the lasing modes in these mirrorless lasers [9]. In the regime of Anderson localization, the lasing modes are predicted to build upon the Anderson-localized modes of the passive system [7], although this was never confirmed experimentally. This regime

has been proposed to obtain low-threshold and stable multimode random lasers [6]. It was further realized that random lasing can also occur in diffusive samples, where modes are spatially extended [10]. Since then, random lasing has been observed and studied in a large variety of systems ranging from π -conjugated polymers [11] to optofluidic systems [12], and from fiber lasers [13–15], bio-polymer film [16], and silkworm silk fibers [17] to planar nanophotonic networks [18], to cite a few. But in most cases, scattering was not strong enough to operate in the localized regime. Or at least, localization could not be demonstrated directly. In this context, an unambiguous experimental demonstration of random lasing in the regime of Anderson localization was yet missing. It was first investigated in a stack of microscope cover slides with active dye [19], and later in Er-doped random Bragg grating fiber [20], where a low-threshold laser emission was assumed to occur on long-lived modes overlapping spatially with the gain region, yet without identification of the nature of the modes. Lasing modes localized over only a few camera pixels were directly observed in disordered photonic crystal waveguides embedded with quantum dots [21], while the cavity mode volume was inferred in [22] from the laser input–output characteristic, by relying on a theoretical model of semiconductor laser rate equations [23]. Other indirect methods were proposed earlier to retrieve modal extension, first in [24] with spectrally resolved speckle techniques, and in [25–27] by displacing the pump and monitoring the emission spectrum. In contrast, the exponentially decaying spatial profiles of lasing modes have been directly observed in a jet of dye droplets, using hyper-spectral imaging [28]. However, beside the specificity of the

photonic system, the method itself cannot isolate the modes in a regime of strong mode overlap where the spatial hole burning effect and mode competition for gain are expected to strongly modify the nature of the modes. A method that truly isolates modes is therefore indispensable to investigate their features. The experimental challenge resides not only in the highly multimode nature of random lasers, but also in the complex association of a non-Hermitian scattering system with a strongly nonlinear active medium. Linear and nonlinear modal interaction, strong gain-induced nonlinearities, including gain saturation and cross-saturation, expected in random lasers, makes it even more difficult to extract the actual mode profile from any measurement.

In this paper, we investigate random lasing in a strongly scattering active medium and demonstrate disorder-induced Anderson localization of lasing modes. To address this issue, we design an optically pumped scattering random laser that allows direct imaging of the field intensity distribution within the laser. We propose to pump non-uniformly the random laser to force it in single-mode operation. We expect the spatially modulated pump intensity to excite selectively a particular lasing mode, while rejecting all others below threshold. To find the correct pump profile, if it exists, we inspired ourselves from a method recently proposed based on gain shaping and an iterative optimization algorithm [29]. This method has been successfully demonstrated experimentally to select modes in a weakly scattering random laser [30], in a microdisk laser [31], and in asymmetric resonant cavities [32]. It was also proposed to control spectral characteristics [29,30,33], laser power efficiency [34], emission directionality [31,35], laser threshold [36], and modal interactions [37,38]. Here, we apply this method to select lasing modes individually and image them spatially.

Remarkably, the natural complexity of the active disordered system is disentangled, revealing the localized nature of each lasing mode individually. We test our method by measuring the intensity profile of a large number of laser modes and by computing the probability distribution of the inverse localization length. We demonstrate how hole burning interactions are efficiently suppressed [39], resulting in reduced threshold and large enhancement of slope efficiency. We show how the location of the localized lasing mode is critical to laser power efficiency by identifying the optimally outcoupled modes of the random laser [34]. These findings open a new route to a more systematic exploration of optical localized modes in photonics. This includes the investigation of linear and nonlinear modal interactions [38,40,41] or the role of nonlinearities on localization [42–44], as well as engineering modal confinement to control mode competition [37,45] or to explore new states of disordered matter in the presence of gain [46].

2. RESULTS

We have designed a solid-state organic random laser [Fig. 1(a)], which benefits from laser stability, sample longevity, and most importantly for our study, relatively strong scattering, a necessary condition to observe the regime of Anderson localization in a finite-sized sample. Once polymerized, a 600-nm-thick layer of doped-polymer (DCM-doped PMMA) spin-coated on a fused silica plate is structured by engraving hundreds of parallel randomly spaced air-grooves, using electron-beam lithography. Controlled disorder is introduced by varying the groove position around a periodic arrangement. A typical mask and a section of the sample are shown in Figs. 1(c) and 1(b). A SEM image is taken after removing a layer of polymer along the sample length to have a clear

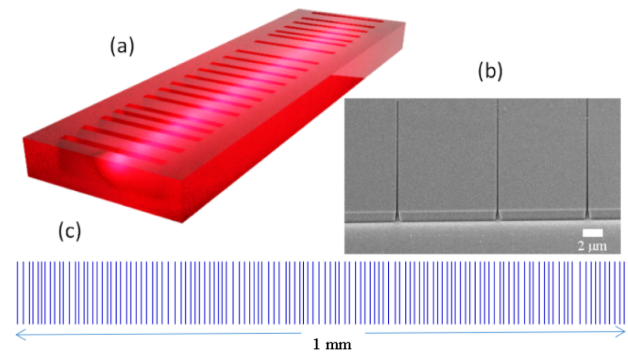


Fig. 1. The solid-state random laser is based on a (DCM) dye-doped 600-nm-thick layer of polymer (PMMA) spin-coated on fused silica. The scattering is provided by 125 parallel grooves (600 nm deep, 350 nm wide on average, 50 μm long) randomly distributed along the 1-mm-long sample with an average period of 8 μm . (a) Artist view of the random laser, which is optically pumped from below by a laser strip line. (b) After removing a layer of polymer along the length of the sample, high-resolution scanning electron microscope (SEM) image of the photonic system taken at 52° angle, showing a cross section of the carved air-grooves. Part of the polymer layer has been removed to show the cross section of the groove (c) Lithographic mask for a particular disorder realization.

view of the carved grooves' cross section. The fabrication process is inspired from the method developed for organic microlasers in [47] and is described in full details in Supplement 1 Section A. When optically pumped (from below) at 532 nm, spontaneously emitted light guided within the polymer film is scattered at the grooves' interface and amplified as it propagates perpendicular to them, along the sample length. Finally, the degree of scattering and, consequently, the localization length, can be adjusted by varying the depth of the grooves. In the present study, the scattering system is composed of 125 identical parallel grooves, uniformly distributed around an 8- μm -pitch periodic lattice with deviation of $\pm 3 \mu\text{m}$ [Fig. 1(c)]. Each groove is 600 nm deep, 50 μm long, and 350 nm wide. The total length of the sample is $L = 1000 \mu\text{m}$. Although a similar design is possible in two dimensions, quasi-1D geometry was preferred here to increase the return probability and the chances to observe localization within the geometric limit of our sample.

We estimate numerically the localization length in our sample, using a simplified 1D-layered model and the transmission matrix method. The localization length ξ is obtained from the average over a large collection of disordered configurations of the logarithm of the transmission, $\xi = \langle \ln T(L) \rangle$, where L is the sample length (for details, see Supplement 1 Section B). It is found to be $\xi = 65 \mu\text{m}$, well within the geometric limits of our sample. We also performed a more realistic full-2D numerical modeling of the passive system, based on finite-element method [COMSOL-Multiphysics with a radio frequency (RF) module], which includes all sample layers and groove geometry.

The field intensity distribution along the waveguide is shown in Fig. 2(c). A close-up view reveals the complexity of both in-plane and out-of-plane scattering. The structuration of the sample offers actually an extra bonus: out-of-plane scattering into air allows imaging of the laser intensity profile close to the sample surface, otherwise confined by the waveguide geometry. Here we can safely assume that this image reproduces in-plane intensity within the sample. This is confirmed in Figs. 2(a) and 2(b), which compare the intensity distribution of a particular localized mode within

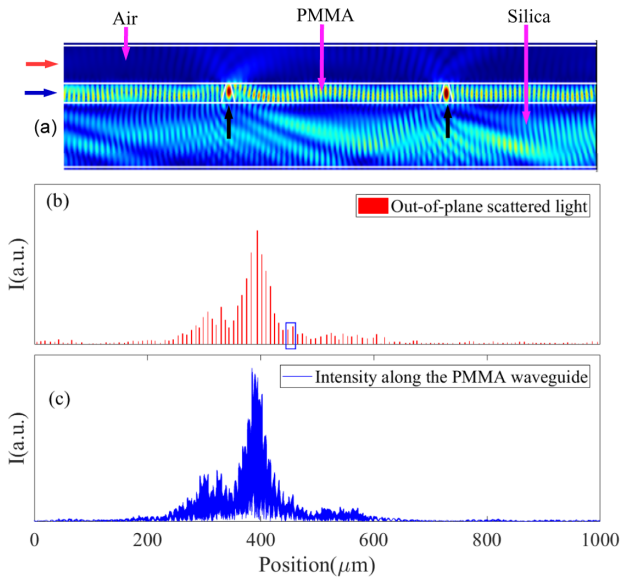


Fig. 2. Full-2D numerical simulation of the field intensity distribution (first mode) of the resonance at $\lambda_0 = 601$ nm (frequency $f = 4.99 \times 10^{14} + i9.7 \times 10^{11}$ Hz), calculated for a 1000 μm -long sample with 125 grooves randomly distributed. The sample geometry is reproduced. Thickness of PMMA/DCM layer, air layer, and silica substrate are, respectively, 600 nm, 1200 nm, and 2000 nm. Their respective refractive indices are $n = 1.54$, $n_{\text{air}} = 1$, and $n_{\text{Silica}} = 1.44$. We use a perfectly matched layer (PML) after air and silica substrate. (a) Electric field intensity distribution computed in the vicinity of two slanted grooves; upward black arrow shows positions of grooves [identified by the blue box in (b)]. (b) Intensity profile of the light scattered by the grooves calculated just above the waveguide (red arrow). (c) Intensity profile along the waveguide (blue arrow) for the localized mode shown in (b).

the waveguide [Fig. 2(c)] to the intensity scattered by the groove, just above the sample [Fig. 2(b)]. The image of the scattered field intensity accurately reproduces the intensity profile of the mode. It is therefore possible to retrieve the spatial profile of the mode from measurement of the out-of-plane scattered light, a useful advantage offered by this system.

A laser strip (500 $\mu\text{m} \times 50 \mu\text{m}$) from a frequency-doubled Nd:YAG laser at 532 nm is used to pump uniformly the random structure. The experimental setup is described in Fig. 3. At laser energy above 18 nJ, multiple scattering provides the necessary optical feedback to reach laser oscillations, and sharp discrete peaks appear on a broad spontaneous emission (SE) background [inset Fig. 4(c)]. As it is most often the case with random lasers, emission is multimode. The out-of-plane laser radiation is imaged under a $\times 10$ microscope objective [Fig. 4(a)], showing out-of-plane scattered light at the position of the air-grooves, in contrast to uniformly distributed SE detected below threshold [Fig. 4(b)].

By monitoring independently and simultaneously laser intensity and SE, we observe the clamping of SE. This feature, which occurs when stimulated emission becomes the preferred transition mechanism, is a fundamental signature of lasing [48,49]. To the best of our knowledge, it has never been observed for random lasers. It is shown in Figs. 4(b) and 4(c), where the growth of SE is seen to be drastically curtailed as the threshold is reached and laser oscillations take over.

The field intensity distribution is recovered after subtracting the SE contribution. This procedure is detailed in Supplement 1 Section C. A typical intensity profile of laser emission when

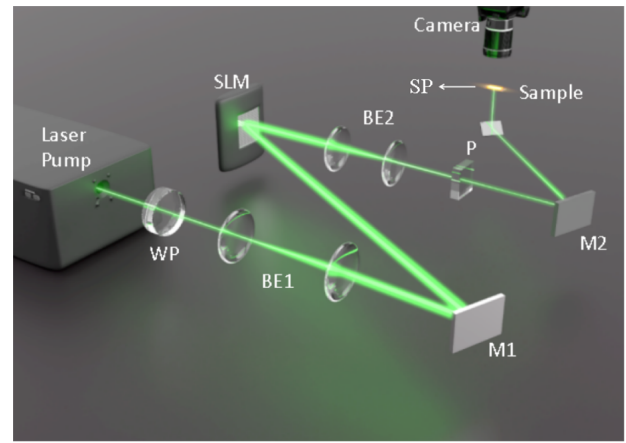


Fig. 3. Schematics of the experimental setup. The 532-nm beam of a 28-ps frequency-doubled mode-locked Nd:YAG laser is first expanded on a computer-driven LCOS amplitude spatial light modulator (SLM), which offers the possibility to modulate spatially the pump intensity. The reflected laser pattern is demagnified and imaged on the back of the sample. A fixed-stage optical microscope (not represented) magnifies ($10\times$) the field intensity scattered at the surface of the sample onto a sCMOS camera. WP, half-wave plate; M1 and M2, mirrors; BE1 and BE2, beam expanders; P, polarizer; SP, spectrometer.

uniformly pumped is shown in Fig. 5(h), corresponding to the multimode emission spectrum shown in Fig. 5(a). Several modes contribute to this profile, preventing any investigation of their spatial distribution individually. To observe them separately, we propose to operate the random laser in single mode at the lasing wavelength we want to investigate. This is achieved by tailoring the intensity profile of the pump to excite selectively this particular mode. After reflection on a computer-driven spatial light modulator (SLM), the pump beam is modulated and projected on the backside of the sample (see Fig. 3 and Supplement 1 Section D). Because the pump profile that selects a particular mode is not known a priori, an iterative method based on an optimization algorithm is used following [30] (see Supplement 1 Sections E and F). We first aim at selecting a mode that is not the first mode to lase under uniform pumping at $\lambda = 599.80$ nm. After 200 iterations, a non-uniform pump profile is found [top inset of Fig. 5(i)], which optimally selects the targeted mode lasing wavelength and rejects all others below threshold, as demonstrated in Fig. 5(b). Remarkably, pure single-mode operation is achieved, in contrast to [30], where mode rejection was not total. The out-of plane scattered light is imaged from the top of the sample. The resulting intensity profile is shown in Fig. 5(i). The lasing mode is found to be spatially confined away from the sample limits. This indicates that random lasing indeed occurs in the localized regime. The same operation is reproduced to select other lasing modes from the multimode emission spectrum in Fig. 5(a). For each mode, a new pump profile is systematically found that selects this particular mode. Imaging the selected modes reveals that all lasing modes are spatially localized. Figures 5(b)–5(g) show emission spectra of six individually selected lasing modes and corresponding lasing mode intensity distributions, together with their optimized pump profiles shown in Figs. 5(i)–5(n). Repeating optimization of a particular lasing peak leads in general to different pump profiles. Remarkably, however, the spatial intensity profile of the corresponding mode is found to be unique and independent of the pump profile (for details, see Supplement 1 Section G).

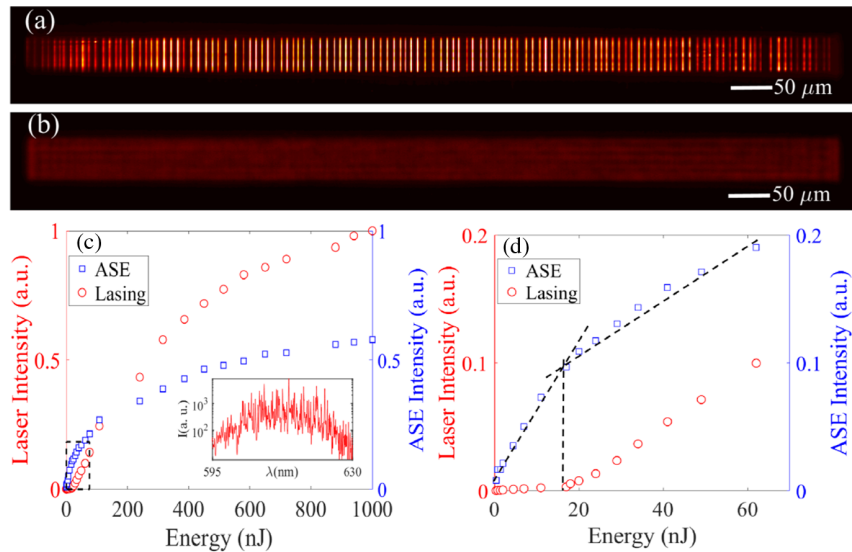


Fig. 4. Optical microscope image of field intensity distribution near the sample surface when pumped (a) above threshold and (b) below threshold. (c) Spontaneous emission (SE) (blue open square) and scattered laser intensity (red open circle) versus pump energy. Inset: emission spectrum with sharp discrete peaks on a broad SE background plotted in semi-log scale. (d) Zoom-in of (c). Clamping of the SE is observed at threshold, for a pump energy of 18 nJ. Note that the laser intensity measured here from out-of-plane scattering is only a small fraction of the actual laser emission, which explains that it is comparable to SE.

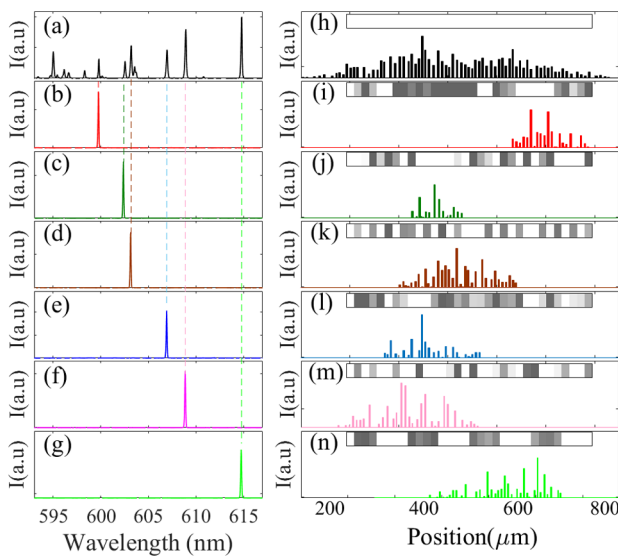


Fig. 5. Selective pumping of localized lasing modes. (a) Random laser emission spectrum obtained in the case of uniform pumping (pump energy is 71.2 nJ). (b)–(g) Emission spectra of selected modes after optimization at target wavelengths: $\lambda = 599.78$ nm, 602.44 nm, 603.17 nm, 606.95 nm, 608.87 nm, and 614.75 nm, respectively. (h) Spatial field intensity distribution corresponding to emission spectrum in (a), measured at the groove positions. Each bar integrates light intensity scattered by one groove. The pump intensity profile is shown on top. (i)–(n) Spatial distribution of laser intensity within the random structure corresponding to each individually selected mode shown in left panel. The corresponding optimized pump profile is reproduced in gray scale on top of each figure (white: maximum intensity; black: no pumping). The spectral mode rejections w.r.t. maximum noise level in the spectra obtain with this method are 56.18 dB, 64.49 dB, 60.56 dB, 58.72 dB, 66.41 dB, and 69.87 dB, respectively.

Lasing modes are found to be exponentially localized in different regions of the sample and occupy a significant fraction of the

sample length. Despite strong spatial overlap, it is possible to measure their spatial extension. The relatively easy access to the spatial distribution of individual localized modes allows us to explore the probability distribution of their localization length. Its inverse, which is the Lyapunov exponent, is expected to follow a normal distribution in a sufficiently long 1D random system with weak disorder [50]. Deviation from normal distribution, when a far tail becomes significant, can be induced by, e.g., the different nature of the states [51], disorder correlation [52], or absorption [53]. Such a deviation has been at the center of a strong debate, as it is directly related to the breakdown of single-parameter scaling theory, which is one of the foundations of localization theory [54]. Here, we measured the mode extension for 75 lasing modes individually selected in 10 samples with different disordered configurations. All samples were carefully manufactured under identical conditions. We define the mode's length as the distance between the extreme scattering grooves from which intensity of light scattered is above noise level. The inverse mode length [50] probability distribution is plotted in Fig. 6, together with a normal fit. A tail to the distribution indicates departure from normal distribution. Half of the mean value of distribution gives the average localization length, $\xi = 100 \mu\text{m}$. The inset in Fig. 6 shows the intensity profile of a localized mode in log scale. Exponential decay is not always as sharply defined as in this case. We use therefore the spatial mode extension to estimate localization length.

We further point out here that the optimization algorithm does not trivially converge to a narrow pump profile near the center of the mode, which would have been sufficient to select spatially isolated and strongly confined modes [7,29]. Here, the distribution of the pump intensity extends far beyond the center of the mode. The reason for this non-trivial optimal pump profile is that modes overlap significantly in our system and therefore compete for gain. Optimal selection of a single lasing mode necessitates therefore to disentangle interacting modes. This is achieved by suppressing the hole burning effect and turning off cross-saturation. The ability of pump shaping to isolate each mode individually is remarkably

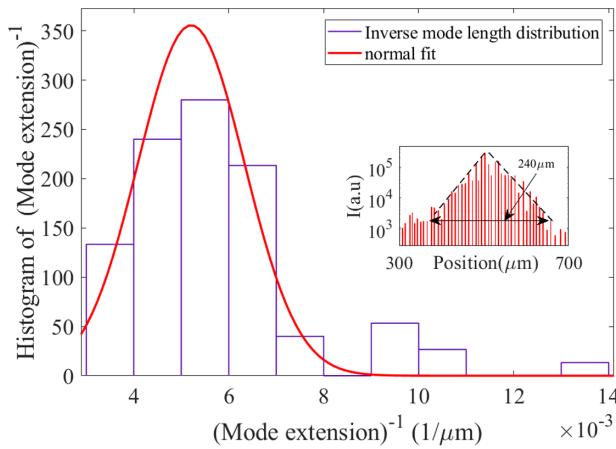


Fig. 6. Histogram of the inverse mode spatial extension probability distribution calculated for 75 different lasing modes, selected individually. Solid red line is normal fit. Inset shows spatial field distribution of a localized mode in log scale.

demonstrated in Fig. 7, which compares the laser characteristic of the mode at 599.78 nm for a uniform and optimized pump profile. When the system is pumped uniformly (multimode regime), the targeted-mode emission at 599.78 nm saturates rapidly, impeded by mode competition and cross-saturation between different lasing modes. Once optimized, the laser intensity becomes linear with pump energy, confirming that no other mode is lasing simultaneously. The selecting profile is found to be efficient in preventing spatial hole burning, below and far above the pump energy at which the optimization was performed. Strikingly, the threshold of the lasing mode after optimization is reduced by a factor of 1.5, while the slope efficiency of its laser characteristic is increased by a factor of six, when compared to the same mode lasing in a multimode regime under uniform pumping. This means that the energy couples out of the random laser more efficiently when the mode is optimized. The selective method employed here releases the selected mode from competing for gain with other modes. This is an important condition to investigate the nature of localized states,

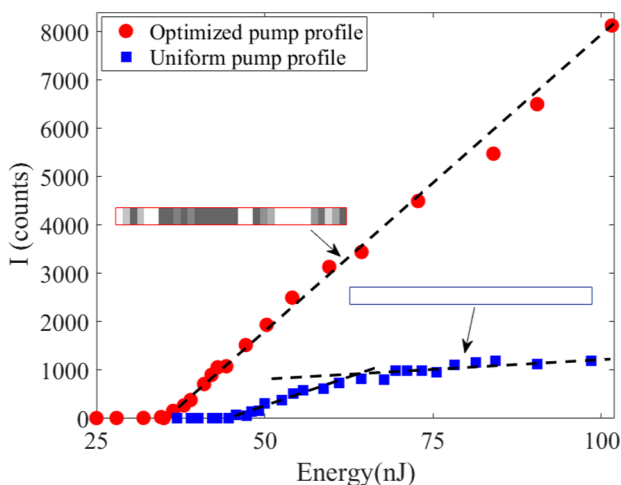


Fig. 7. Laser characteristic (intensity versus pump energy) for the lasing mode at 599.78 nm: (blue full square) in multimode operation (uniform pump profile); (red full circle) in single-mode operation (optimized pump profile). In multimode regime, the threshold of the mode at 599.78 nm is 47.3 nJ, and its slope efficiency is 20 counts/nJ. In single-mode regime, its threshold reduces to 35 nJ, and its slope efficiency increases to 123 counts/nJ.

which other methods, including hyperspectral imaging, may not allow when mode overlap is important. The performance of the laser has therefore been improved by “focusing” the pump where it is needed and consequently reducing the gain surface, a rather counterintuitive effect.

This significant improvement in laser energy efficiency can be pushed even a step further by selecting the optimally outcoupled lasing mode of the random laser. The optimally outcoupled lasing mode of an optical resonator is the mode that provides the largest slope efficiency. It was argued in [34] that such modes are suppressed by spatial hole burning interactions in a uniformly pumped laser. Shaping the pump profile was therefore proposed [34,39] to control spatial hole burning, increase laser stability and laser power efficiency, and allow lasing in the most efficient mode. This was tested numerically in a microdisk laser, where the optimally coupled mode can be calculated and the pump profile is trivial. In a random laser, however, both modal identification and pump selection turn out to be much more challenging. Here, we show how our approach, which couples mode selection and mode imaging, allows to identify the optimally outcoupled modes of our random laser. We measure the threshold and the slope efficiency of 15 individual lasing modes of a given sample, after they have been selectively pumped. Threshold and slope efficiency are then correlated with the position of each mode along the sample, defined here as the position of its barycenter. The laser threshold (red plot in Fig. 8) is seen to grow for modes near the sample boundaries, as leakage out from the scattering medium increases the loss of these modes. Actually, the measure of the threshold provides a direct evaluation of the sensitivity of the localized modes to the boundary of the system [55]. The slope efficiency presented in the blue plot in (Fig. 8) shows a remarkable feature: it exhibits two maxima at positions 200 and 700 μm, almost symmetric around the center of the sample. Maximum slope efficiency defines the optimally outcoupled lasing modes for this particular disordered system. It is worth noting that this happens for lasing modes localized neither near the center of the sample nor near the sample edges. This shows how critical is the spatial position of the optimally outcoupled modes. It is a delicate trade-off between low-loss modes, which build up energy near the center, and efficiently output-coupled modes close to the sample edges. This demonstrates how mode selection by tailoring the pump profile can turn on the most efficient lasing modes of

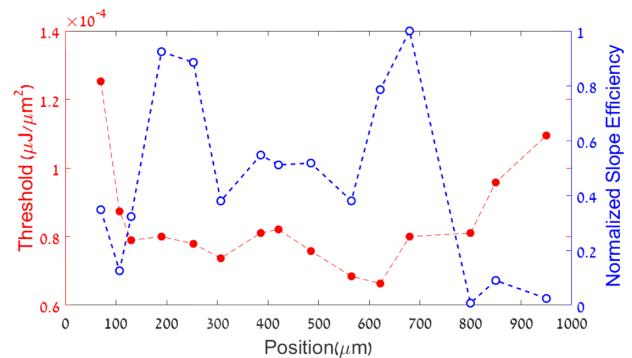


Fig. 8. Lasing threshold (red full circles) and normalized slope efficiency (blue open circles) versus mode position along the sample of individually excited lasing modes. From left to right: $\lambda = 622.12$ nm, 609.02 nm, 605.05 nm, 606.91 nm, 595.48 nm, 604.73 nm, 606.49 nm, 619.04 nm, 614.48 nm, 612.60 nm, 617.15 nm, 606.35 nm, 598.66 nm, 602.74 nm. The position of the mode is defined as the position of its barycenter.

a particular random laser. Our findings extend the theoretical predictions in [34] to the most challenging case of random lasers.

3. CONCLUSION

In conclusion, we have explored random lasing in the strongly scattering regime, and demonstrated disorder-induced localization, by combining selective pump shaping and imaging of individual lasing modes in a newly designed random laser. We confirmed the spatial confinement of all lasing modes and identified the optimally outcoupled modes of the random laser. Selective excitation by non-uniform pumping proves itself remarkably efficient to suppress spatial hole burning, modal interaction, and cross-saturation effect in an otherwise strongly non-Hermitian system. We claim that this method works actually as an effective eigensolver to retrieve localized modes individually and to identify the lasing modes that boost laser efficiency, which is out of reach of other methods found in literature. Our findings can be extended to 2D systems, where localized laser modes are more challenging to achieve. It opens a unique route to investigate Anderson localization, explore the role of nonlinearities on localization, and test experimentally theoretical predictions [42]. It can be applied also to the design of highly efficient and stable random microlasers, where the random and non-Hermitian nature of these lasers offers unprecedented degrees of freedom.

Funding. Israel Science Foundation (1871/15, 2074/15, 2630/20); United States—Israel Binational Science Foundation (2015694); MAFAT (4440938424); Air Force Office of Scientific Research (FA9550-18-1-0208); CNRS, PICS-ALAMO; Planning and Budgeting Committee of the Council for Higher Education of Israel (2015-2018).

Acknowledgment. We thank Profs. V. Freilikher and A. Z. Genack for useful discussions. We are grateful to Dr. Yossi Abulafia for his help in the fabrication process and to Bar-Ilan Institute of Nanotechnology & Advanced Materials for providing fabrication facilities.

Disclosures. The authors declare no conflicts of interest.

Data availability. Data underlying the results presented in this paper are not publicly available at this time but may be obtained from the authors upon reasonable request.

Supplemental document. See Supplement 1 for supporting content.

REFERENCES

- P. W. Anderson, "Absence of diffusion in certain random lattices," *Phys. Rev.* **109**, 1492–1505 (1958).
- S. John, "Electromagnetic absorption in a disordered medium near a photon mobility edge," *Phys. Rev. Lett.* **53**, 2169–2172 (1984).
- P. W. Anderson, "The question of classical localization: a theory of white paint?" *Philos. Mag.* **52**(3), 505–509 (1985).
- B. A. van Tiggelen and S. E. Skipetrov, "Longitudinal modes in diffusion and localization of light," *Phys. Rev. B* **103**, 174204 (2021).
- F. Riboli, N. Caselli, S. Vignolini, F. Intonti, K. Vynck, P. Barthelemy, A. Gerardo, L. Balet, L. H. Li, A. Fiore, M. Gurioli, and D. S. Wiersma, "Engineering of light confinement in strongly scattering disordered media," *Nat. Mater.* **13**, 720–725 (2014).
- X. Jiang and C. M. Soukoulis, "Localized random lasing modes and a path for observing localization," *Phys. Rev. E* **65**, 025601 (2001).
- C. Vanneste and P. Sebbah, "Selective excitation of localized modes in active random media," *Phys. Rev. Lett.* **87**, 183903 (2001).
- H. Cao, Y. G. Zhao, S. T. Ho, E. W. Seelig, Q. H. Wang, and R. P. H. Chang, "Random laser action in semiconductor powder," *Phys. Rev. Lett.* **82**, 2278–2281 (1999).
- J. Andreasen, A. A. Asatryan, L. C. Botten, M. A. Byrne, H. Cao, L. Ge, L. Labonté, P. Sebbah, A. D. Stone, H. E. Türeci, and C. Vanneste, "Modes of random lasers," *Adv. Opt. Photon.* **3**, 88–127 (2011).
- C. Vanneste, P. Sebbah, and H. Cao, "Lasing with resonant feedback in the diffusive regime," *Phys. Rev. Lett.* **98**, 183903 (2007).
- A. Tulek, R. Polson, and Z. A. Vardeny, "Naturally occurring resonators in random lasing of π -conjugated polymer films," *Nat. Phys.* **6**, 303–310 (2010).
- N. S. Bhaktha, N. Bachelard, X. Noblin, and P. Sebbah, "Optofluidic random laser," *Appl. Phys. Lett.* **101**, 151101 (2012).
- C. J. S. de Matos, L. S. Menezes, A. M. Brito-Silva, M. A. M. Gámez, A. S. L. Gomes, and C. B. de Araújo, "Random fiber laser," *Phys. Rev. Lett.* **99**, 153903 (2007).
- S. K. Turitsyn, S. A. Babin, A. E. El-Taher, P. Harper, D. V. Churkin, S. I. Kablukov, J. D. A. Castañón, V. Karalekas, and E. V. Podivilov, "Random distributed feedback fibre laser," *Nat. Photonics* **4**, 231–235 (2010).
- M. Leonetti, S. Karbasi, A. Maffi, and C. Conti, "Observation of migrating transverse Anderson localizations of light in nonlocal media," *Phys. Rev. Lett.* **112**, 193902 (2014).
- A. Consoli, E. Soria, N. Caselli, and C. López, "Random lasing emission tailored by femtosecond and picosecond pulsed polymer ablation," *Opt. Lett.* **44**, 518–521 (2019).
- S. H. Choi, S.-W. Kim, Z. Ku, M. A. Visbal-Onufrak, S.-R. Kim, K.-H. Choi, H. Ko, W. Choi, A. M. Urbas, T.-W. Goo, and Y. L. Kim, "Anderson light localization in biological nanostructures of native silk," *Nat. Commun.* **9**, 452 (2018).
- M. Gaio, D. Saxena, J. Bertolotti, D. Pisignano, A. Camposeo, and R. Sapienza, "A nanophotonic laser on a graph," *Nat. Commun.* **10**, 226 (2019).
- V. Milner and A. Z. Genack, "Photon localization laser: low-threshold lasing in a random amplifying layered medium via wave localization," *Phys. Rev. Lett.* **94**, 073901 (2005).
- M. Gagné and R. Kashyap, "Demonstration of a 3 mW threshold Er-doped random fiber laser based on a unique fiber Bragg grating," *Opt. Express* **17**, 19067–19074 (2009).
- J.-K. Yang, H. Noh, M. J. Rooks, G. S. Solomon, F. Vollmer, and H. Cao, "Lasing in localized modes of a slow light photonic crystal waveguide," *Appl. Phys. Lett.* **98**, 241107 (2011).
- J. Liu, P. D. Garcia, S. Ek, N. Gregersen, T. Suhr, M. Schubert, J. Mørk, S. Stobbe, and P. Lodahl, "Random nanolasing in the Anderson localized regime," *Nat. Nanotechnol.* **9**, 285–289 (2014).
- N. Gregersen, T. Suhr, M. Lorke, and J. Mørk, "Quantum-dot nanocavity lasers with Purcell-enhanced stimulated emission," *Appl. Phys. Lett.* **100**, 131107 (2012).
- H. Cao, Y. Ling, J. Y. Xu, and A. L. Burin, "Probing localized states with spectrally resolved speckle techniques," *Phys. Rev. E* **66**, 025601 (2002).
- K. L. Van der Molen, R. W. Tjerkstra, A. P. Mosk, and A. Lagendijk, "Spatial extent of random laser modes," *Phys. Rev. Lett.* **98**, 143901 (2007).
- R. C. Polson and Z. V. Vardeny, "Spatially mapping random lasing cavities," *Opt. Lett.* **35**, 2801–2803 (2010).
- R. G. S. El-Dardiry, A. P. Mosk, O. L. Muskens, and A. Lagendijk, "Experimental studies on the mode structure of random lasers," *Phys. Rev. A* **81**, 043830 (2010).
- R. Kumar, M. Balasubrahmaniam, K. S. Alee, and S. Mujumdar, "Temporal complexity in emission from Anderson localized lasers," *Phys. Rev. A* **96**, 063816 (2017).
- N. Bachelard, J. Andreasen, S. Gigan, and P. Sebbah, "Taming random lasers through active spatial control of the pump," *Phys. Rev. Lett.* **109**, 033903 (2012).
- N. Bachelard, S. Gigan, X. Noblin, and P. Sebbah, "Adaptive pumping for spectral control of random lasers," *Nat. Phys.* **10**, 426–431 (2014).
- S. F. Liew, B. Redding, L. Ge, G. S. Solomon, and H. Cao, "Active control of emission directionality of semiconductor microdisk lasers," *Appl. Phys. Lett.* **104**, 231108 (2014).
- F. Gu, F. Xie, X. Lin, S. Linghu, W. Fang, H. Zeng, L. Tong, and S. Zhuang, "Single whispering-gallery mode lasing in polymer bottle microresonators via spatial pump engineering," *Light Sci. Appl.* **6**, e17061 (2017).
- Y. Qiao, Y. Peng, Y. Zheng, F. Ye, and X. Chen, "Adaptive pumping for spectral control of broadband second-harmonic generation," *Opt. Lett.* **43**, 787–790 (2018).
- L. Ge, O. Malik, and H. E. Türeci, "Enhancement of laser power-efficiency by control of spatial hole burning interactions," *Nat. Photonics* **8**, 871–875 (2014).

35. T. Hisch, M. Liertzer, D. Pogany, F. Mintert, and S. Rotter, "Pump-controlled directional light emission from random lasers," *Phys. Rev. Lett.* **111**, 023902 (2013).
36. J.-H. Choi, S. Chang, K.-H. Kim, W. Choi, S.-J. Lee, J. M. Lee, M.-S. Hwang, J. Kim, S. Jeong, M.-K. Seo, W. Choi, and H.-G. Park, "Selective pump focusing on individual laser modes in microcavities," *ACS Photon.* **5**, 2791–2798 (2018).
37. A. Cerjan, B. Redding, L. Ge, S. F. Liew, H. Cao, and A. D. Stone, "Controlling mode competition by tailoring the spatial pump distribution in a laser: a resonance-based approach," *Opt. Express* **24**, 26006–26015 (2016).
38. L. Ge, "Selective excitation of lasing modes by controlling modal interactions," *Opt. Express* **23**, 30049–30056 (2015).
39. Z. Zhang, P. Miao, J. Sun, S. Longhi, N. M. Litchinitser, and L. Feng, "Elimination of spatial hole burning in microlasers for stability and efficiency enhancement," *ACS Photon.* **5**, 3016–3022 (2018).
40. J. Andreasen, P. Sebbah, and C. Vanneste, "Nonlinear effects in random lasers," *J. Opt. Soc. Am. B* **28**, 2947–2955 (2011).
41. H. E. Türeci, L. Ge, S. Rotter, and A. D. Stone, "Strong interactions in multimode random lasers," *Science* **320**, 643–646 (2008).
42. P. Stano and P. Jacquod, "Suppression of interactions in multimode random lasers in the Anderson localized regime," *Nat. Photonics* **7**, 66–71 (2013).
43. T. Schwartz, G. Bartal, S. Fishman, and M. Segev, "Anderson localization in disordered two-dimensional photonic lattices," *Nature* **446**, 52–55 (2007).
44. Y. Lahini, A. Avidan, F. Pozzi, M. Sorel, R. Morandotti, D. N. Christodoulides, and Y. Silberberg, "Anderson localization and non linearity in one-dimensional disordered photonic lattices," *Phys. Rev. Lett.* **100**, 013906 (2008).
45. H. Cao, X. Jiang, Y. Ling, J. Y. Xu, and C. M. Soukoulis, "Mode repulsion and mode coupling in random lasers," *Phys. Rev. B* **67**, 161101 (2003).
46. S. Yu, C.-W. Qiu, Y. Chong, S. Torquato, and N. Park, "Engineered disorder in photonics," *Nat. Rev. Mater.* **6**, 226–243 (2021).
47. M. Leubental, N. Djellali, C. Arnaud, J.-S. Lauret, J. Zyss, R. Dubertrand, C. Schmit, and E. Bogomolny, "Inferring periodic orbits from spectra of simply shaped microlasers," *Phys. Rev. A* **76**, 023830 (2007).
48. M. J. Marell, B. Smalbrugge, E. J. Geluk, P. J. van Veldhoven, B. Barcones, B. Koopmans, R. Nötzel, M. K. Smit, and M. T. Hill, "Plasmonic distributed feedback lasers at telecommunications wavelengths," *Opt. Express* **19**, 15109–15118 (2011).
49. T. Burgess, D. Saxena, S. Mokkaapati, Z. Li, C. R. Hall, J. A. Davis, Y. Wang, L. M. Smith, L. Fu, P. Caroff, H. H. Tan, and J. Chennupati, "Doping-enhanced radiative efficiency enables lasing in unpassivated GaAs nanowires," *Nat. Commun.* **7**, 11927 (2016).
50. V. D. Freilikher and S. A. Gredeskul, "Localization of waves in media with one-dimensional disorder," *Prog. Opt.* **30**, 137–203 (1992).
51. L. I. Deych, D. Zaslavsky, and A. A. Lisyansky, "Statistics of the Lyapunov exponent in 1D random periodic-on-average systems," *Phys. Rev. Lett.* **81**, 5390–5393 (1998).
52. E. Gurevich and A. Iomin, "Generalized Lyapunov exponent and transmission statistics in one-dimensional Gaussian correlated potentials," *Phys. Rev. E* **83**, 011128 (2011).
53. L. I. Deych, A. Yamilov, and A. A. Lisyansky, "Scaling in one-dimensional localized absorbing systems," *Phys. Rev. B* **64**, 024201 (2001).
54. E. Abrahams, P. W. Anderson, D. C. Licciardello, and T. V. Ramakrishnan, "Scaling theory of localization: absence of quantum diffusion in two dimensions," *Phys. Rev. Lett.* **42**, 673–676 (1979).
55. J. T. Edwards and D. J. Thouless, "Numerical studies of localization in disordered systems," *J. Phys. C* **5**, 807–820 (1972).